Construction of Smooth Maps with Mean Value Coordinates

Torsten Langer   Hans-Peter Seidel

MPI–I–2007–4–002   May 2007

Authors' Addresses

Torsten Langer
Max-Planck-Institut für Informatik
Stuhlsatzenhausweg 85
66123 Saarbrücken
Germany

Hans-Peter Seidel
Max-Planck-Institut für Informatik
Stuhlsatzenhausweg 85
66123 Saarbrücken
Germany

Acknowledgements

We want to thank Alexander Belyaev for helpful discussions. The research of the authors has been supported in part by the EU-Project "AIM@SHAPE" FP6 IST Network of Excellence 506766.

Abstract

Bernstein polynomials are a classical tool in Computer Aided Design to create smooth maps with a high degree of local control. They are used for the construction of Bézier surfaces, free-form deformations, and many other applications. However, classical Bernstein polynomials are only defined for simplices and parallelepipeds. These can in general not directly capture the shape of arbitrary objects. Instead, a tessellation of the desired domain has to be done first.

We construct smooth maps on arbitrary sets of polytopes such that the restriction to each of the polytopes is a Bernstein polynomial in mean value coordinates (or any other generalized barycentric coordinates). In particular, we show how smooth transitions between different domain polytopes can be ensured.

Keywords

Mean value coordinates, Bézier map, Bézer surface, deformation

Contents

1 Introduction

Bernstein polynomials are at the core of classical Computer Aided Design. In the 1960s, they were used for the construction of Bézier surfaces [1, 2, 6], which remain an important tool until today. Later, Bernstein polynomials were applied to define free-form deformations of 3D space [17]. More general, they can be used to construct any kind of smooth map that requires local control.

In this paper, we use the notion of *Bézier maps* to denote polynomial functions $f : \mathbb{R}^d \to \mathbb{R}^e$ in the form of simplicial Bézier maps

$$f(\lambda) = \sum_{|\alpha|=n} b_\alpha B^n_\alpha(\lambda) \tag{1.1}$$

or tensor product Bézier maps

$$f(\mathbf{x}) = \sum_{i_1,\dots i_d=0}^{n} b_{i_1\dots i_d} \prod_{j=1}^{d} B^n_{i_j}(x_j) \tag{1.2}$$

where $\lambda := \lambda(\mathbf{x})$ are the barycentric coordinates of $\mathbf{x} := (x_1, \dots x_d)$ with respect to a domain simplex (or polytope) $P \subset \mathbb{R}^d$ with vertices $\{\mathbf{v}_1, \dots \mathbf{v}_k\}$ ($k = d + 1$ if P is a simplex) while (1.2) is defined over the domain $[0, 1]^d$. n is the polynomial degree, $b_\alpha \in \mathbb{R}^e$ and $b_{i_1\dots i_d} \in \mathbb{R}^e$ are the control points, and B^n_α and B^n_i are the Bernstein polynomials defined by

$$B^n_\alpha(\lambda) = \frac{n!}{\alpha!}\lambda^\alpha , \qquad B^n_i(x) = \binom{n}{i}(1-x)^{n-i}x^i \tag{1.3}$$

where we use the standard multi-index notation $\alpha := (\alpha_1, \dots \alpha_k) \in \mathbb{N}^k$ with $|\alpha| := \sum_i \alpha_i$, $\alpha! := \prod_i \alpha_i!$, and $\lambda^\alpha := \prod_i \lambda_i^{\alpha_i}$.

Important special cases of Bézier maps are on the one hand Bézier curves and (hyper-)surfaces where $e > d$ and usually $d = 1$ or $d = 2$. On the other hand, if $d = e$, we obtain space deformations. Sederberg and Parry [17] used tensor product Bernstein polynomials defined on parallelepipeds in $\mathbb{R}^3$ to specify such free-form deformations. In this case, the control points b_{ijk} indicate the position and shape of the deformed parallelepiped. However, the restriction on the shape of the domain makes it sometimes difficult to adapt the deformation to complex real objects. This restriction can be overcome by generalizing the barycentric coordinates λ_i in (1.1) from triangles to more general polygons and polyhedra. A first step in this direction was done by Loop and DeRose [15] who introduced coordinate functions l_i in order to define Bézier surfaces over regular k-gons. These coordinates are a special case of the Wachspress coordinates [18] that are defined inside of arbitrary convex polygons and were introduced to computer graphics by Meyer et al. [16]. A further generalization led to the definition of Wachspress coordinates for convex polytopes of higher dimensions [19, 11].

Another generalization of barycentric coordinates, the mean value coordinates, was suggested by Floater [3] and extended to higher dimensions later on [5, 10, 12]. They have the advantage of being defined for arbitrary, convex and non-convex, polytopes. Unfortunately, mean value coordinates are only C^0-continuous at vertices [8]. Langer and Seidel addressed the latter problem and showed that the higher order discontinuities at the vertices vanish in the context of Bézier maps if the control points b_α satisfy certain continuity constraints [14]. They pointed out that mean value Bézier maps have a greater number of control points, and hence greater flexibility, than traditional Bézier maps. Their solution, however, is only valid for Bézier maps defined on a square. Thus, the mean value coordinates lost their greatest strength: to be defined with respect to arbitrary polytopes.

When constructing a smooth map consisting of several polynomials that are defined on adjoining polytopes, we have to ensure that the respective polynomials connect smoothly. For connecting simplicial and tensor product polynomials, a well developed theory is available. In [15], it is shown how regular k-gons and triangles can be smoothly connected if Bernstein polynomials in Wachspress coordinates are used. Unfortunately, their proof requires coordinates that are rational polynomial functions, which is not the case for mean value coordinates. Therefore, it cannot be carried over to mean value Bézier maps (Bézier maps based on mean value coordinates).

In this paper, we derive constraints on the control points of Bézier maps in arbitrary generalized barycentric coordinates to obtain smooth transitions between arbitrary domain polytopes. One essential requirement, as noted in [7], is to adopt an indexing scheme that is adapted to the given polytopes. We chose to use multi-indices (as has been done before in [15]). They correspond to the Minkowski sum approach in [7].

2 Theoretical foundation

Classical barycentric coordinates specify local coordinates $\lambda_i(\mathbf{x})$ for a point $\mathbf{x}$ with respect to a simplex. When generalizing this concept from simplices to arbitrary polytopes P with vertices $\{\mathbf{v}_1 \dots \mathbf{v}_k\}$, we require that the λ_i satisfy

$$\sum_i \lambda_i(\mathbf{x}) = 1 \qquad \text{partition of unity,} \tag{2.1}$$

$$\sum_i \lambda_i(\mathbf{x})\mathbf{v}_i = \mathbf{x} \qquad \text{linear precision.} \tag{2.2}$$

We call a set of continuous functions $\lambda_i(\mathbf{x})$ that satisfies (2.1) and (2.2) *barycentric coordinates*. They are *positive* if additionally

$$\forall i \; \lambda_i(\mathbf{x}) > 0 \qquad \text{positivity} \tag{2.3}$$

holds for all points $\mathbf{x}$ within convex polytopes.

Barycentric coordinates for polytopes can be inserted in (1.1) to obtain (generalized) Bézier maps. Wachspress coordinates and mean value coordinates are the most prominent positive barycentric coordinates. An overview of other coordinates can be found in [4, 9, 12]. It has been observed [15] that Bézier maps based on Wachspress coordinates defined on a square lead to the well-known tensor product Bézier maps. Mean value Bézier maps have the advantage that their domain is not restricted to convex polygons. For all kinds of Bézier maps the following properties are satisfied.

2.1 Proposition. *Let λ_i be barycentric coordinates with respect to a polytope P, and let the Bernstein polynomials B^n_α and a Bézier map f be defined as in (1.3) and (1.1). Then the following properties hold:*

1. $B^n_\alpha(\lambda) = \sum_{i=1}^k \lambda_i B^{n-1}_{\alpha-\mathbf{e}_i}(\lambda)$ *(we set $B^m_\beta(\lambda) := 0$ if one of the $\beta_i < 0$),*
2. *let $(\mathbf{v}_{i_0}, \mathbf{v}_{i_1})$ be an edge of P, then the boundary curve $f(\lambda((1-t)\mathbf{v}_{i_0} + t\mathbf{v}_{i_1}))$ is a Bézier curve with control points $(b_{(n-j)\mathbf{e}_{i_0}+j\mathbf{e}_{i_1}})_{j=0}^n$,*

3. *$\{B^n_\alpha\}$ forms a partition of unity; it is a positive partition of unity within P if P is convex and the λ_i are positive coordinates,*

4. *the image of P under $f(\lambda(\mathbf{x}))$ is contained in the convex hull of the b_α if P is convex and the λ_i are positive coordinates,*

5. *the de Casteljau algorithm works: let $f(\lambda) = \sum_{|\alpha|=n} b_\alpha B^n_\alpha(\lambda)$ be a Bézier map with coefficients b_α. For $m \in \mathbb{N}$ and a given β with $|\beta| = n - m$, let $b^m_\beta(\lambda) := \sum_{|\alpha|=m} b_{\beta+\alpha} B^m_\alpha(\lambda)$. Then $P(\lambda) = b^n_{\mathbf{0}}(\lambda)$ can be computed from the $b^0_\beta(\lambda) = b_\beta$ via the recursive relation $b^m_\beta(\lambda) = \sum_{i=1}^k \lambda_i b^{m-1}_{\beta+\mathbf{e}_i}(\lambda)$.*

($\mathbf{e}_i$ denotes the multi-index with components $(\mathbf{e}_i)_j = \delta_{ij}$, and $\mathbf{0}$ denotes the multi-index with components $\mathbf{0}_j = 0$.)

To join several Bézier maps smoothly, it is important to know their derivatives. In the remainder of the paper, we will assume that the λ_i are differentiable everywhere apart from the vertices $\mathbf{v}_i$. This is in particular true for Wachspress and mean value coordinates. Using the chain rule, it is straightforward to obtain

2.2 Lemma. *Let*

$$f(\lambda) = \sum_{|\alpha|=n} b_\alpha B^n_\alpha(\lambda) . \tag{2.4}$$

Then the first derivatives of f are given by

$$\frac{\partial}{\partial x_i} f(\lambda(\mathbf{x})) = n \sum_{|\alpha|=n-1} \sum_{j=1}^{k} \frac{\partial}{\partial x_i} \lambda_j(\mathbf{x}) b_{\alpha+\mathbf{e}_j} B^{n-1}_\alpha(\lambda(\mathbf{x})) . \tag{2.5}$$

However, the derivatives $\frac{\partial}{\partial x_i}\lambda_j$ are in general not easy to compute. Nevertheless, in [14], constraints on the control points b_α to achieve smooth derivatives across common (hyper-)faces of polytopes have been derived without exact knowledge of the derivatives of λ_j. However, the proof is based on properties of barycentric coordinates that are specific to coordinates defined in a square. Since we want to have smooth transitions of Bézier maps defined on arbitrary polytopes, we need a more general approach. In the following, we give sufficient conditions for the control points b_α to join arbitrary polytopes smoothly.

Basically, the control points at the common (hyper-)faces and adjacent to it must be determined by affine functions A_β and these functions must coincide across these faces. This is visualized in Figure 3.1. The figure shows a Bézier surface and its control net from several viewpoints. The domain consists of a pentagon and an L-shaped hexagon that share two common edges (shown in black below the surface). On the right, the control net is colored to indicate the smoothness conditions. The parts of the control net that correspond to the three common vertices of the two polygons are affine images of the domain polygons. They are colored in blue, red, and green, respectively.

We make this idea more precise in the following theorems. We begin by expressing the derivatives of a Bézier map with respect to the control points.

2.3 Theorem. *Let $f(\lambda) = \sum_{|\alpha|=n} b_\alpha B^n_\alpha(\lambda)$ be a Bézier map defined with respect to a polytope P with vertices $\mathbf{v}_i$. Assume that for every multi-index β with $|\beta| = n-1$ an affine function A_β exists such that $b_\alpha = A_\beta(\sum_i \frac{\alpha_i}{n}\mathbf{v}_i)$ for all pairs α and β such that $\alpha = \beta + \mathbf{e}_j$.*

Then, the derivative of f with respect to a differential operator $\partial \in \left\{\frac{\partial}{\partial x_i}\right\}$ is

$$\partial f(\lambda(\mathbf{x})) = \sum_{|\beta|=n-1} \partial A_\beta \cdot B^{n-1}_\beta(\lambda(\mathbf{x})).$$

Proof. In the following calculation, we use the derivative of f (Lemma 2.2), the definition of A_β, the affine linearity of A_β, the linearity of ∂, again the affine linearity of A_β, partition of unity (2.1) and linear precision (2.2) for $\lambda(\mathbf{x})$ (but note that we suppress $\mathbf{x}$ in the notation otherwise), and that the derivative of a constant is zero.

$$\begin{aligned}
\partial f(\lambda) &= n \sum_{|\beta|=n-1} \sum_{i=1}^{k} \partial\lambda_i b_{\beta+\mathbf{e}_i} B^{n-1}_\beta(\lambda) \\
&= n \sum_{|\beta|=n-1} \sum_{i=1}^{k} \partial\lambda_i A_\beta\Big(\sum_j \frac{\beta_j}{n}\mathbf{v}_j + \frac{1}{n}\mathbf{v}_i\Big) B^{n-1}_\beta(\lambda) \\
&= n \sum_{|\beta|=n-1} \sum_{i=1}^{k} \partial\lambda_i \left(\sum_j \frac{\beta_j}{n} A_\beta(\mathbf{v}_j) + \frac{1}{n} A_\beta(\mathbf{v}_i)\right) B^{n-1}_\beta(\lambda) \\
&= \sum_{|\beta|=n-1} B^{n-1}_\beta(\lambda)\partial\left(\sum_j \beta_j \sum_{i=1}^{k} \lambda_i A_\beta(\mathbf{v}_j) + \sum_{i=1}^{k} \lambda_i A_\beta(\mathbf{v}_i)\right) \\
&= \sum_{|\beta|=n-1} B^{n-1}_\beta(\lambda)\partial\left(\sum_j \beta_j A_\beta\Big(\sum_{i=1}^{k} \lambda_i \mathbf{v}_j\Big) + A_\beta\Big(\sum_{i=1}^{k} \lambda_i \mathbf{v}_i\Big)\right) \\
&= \sum_{|\beta|=n-1} B^{n-1}_\beta(\lambda)\partial\left(\sum_j \beta_j A_\beta(\mathbf{v}_j) + A_\beta(\mathbf{x})\right) \\
&= \sum_{|\beta|=n-1} B^{n-1}_\beta(\lambda)\partial A_\beta. \qquad (2.6)
\end{aligned}$$

□

In the same way, we can compute higher derivatives:

2.4 Corollary. *In the situation of Theorem 2.3 assume that for every multi-index* γ *with* $|\gamma| = n-2$ *an affine function* A'_γ *exists such that* $\partial A_\beta = A'_\gamma(\sum_i \frac{\beta_i}{n-1}\mathbf{v}_i)$ *for all pairs* β *and* γ *such that* $\beta = \gamma + \mathbf{e}_j$.

Then, the derivative $\partial'\partial f$ *of* f *with respect to a differential operator* $\partial' \in \left\{\frac{\partial}{\partial x_i}\right\}$ *is*

$$\partial'\partial f(\lambda(\mathbf{x})) = \sum_{|\gamma|=n-2} \partial' A'_\gamma \cdot B^{n-2}_\gamma(\lambda(\mathbf{x})).$$

Respective statements hold for the higher derivatives of f.

Proof. The claim follows immediately from Theorem 2.3 since $\partial f(\lambda(\mathbf{x})) = \sum_{|\beta|=n-1} \partial A_\beta B^{n-1}_\beta(\lambda(\mathbf{x}))$ is a Bézier map with coefficients ∂A_β. □

2.5 Corollary (Smooth mean value Bézier maps). *Let* $f(\lambda) = \sum_{|\alpha|=n} b_\alpha B^n_\alpha(\lambda)$ *be a Bézier map where the* λ_i *are the mean value coordinates with respect to a polytope* P *with vertices* $\mathbf{v}_i$. *Assume that an affine function* A_i *exists such that* $b_{(n-1)\mathbf{e}_i+\mathbf{e}_j} = A_i(\frac{n-1}{n}\mathbf{v}_i + \frac{1}{n}\mathbf{v}_j)$ *for all* j.

Then, the derivative of f *with respect to any differential operator* $\partial \in \left\{\frac{\partial}{\partial x_i}\right\}$ *has a continuous extension to* $\mathbf{v}_i$ *and*

$$\lim_{\mathbf{x}\to\mathbf{v}_i} \partial f(\mathbf{x}) = \partial A_i.$$

Respective statements hold for the higher derivatives of f.

Proof. We observe that the outer sum in (2.6) collapses to a single summand if the limit $\mathbf{x} \to \mathbf{v}_i$ is considered. We obtain the claim from the remaining term. □

Finally, we obtain constraints on the b_α to achieve smooth Bézier maps across common (hyper-)faces of polytopes.

2.6 Corollary (Continuity across polytope boundaries). *Let* $f(\lambda) = \sum_{|\alpha|=n} b_\alpha B^n_\alpha(\lambda)$ *and* $f'(\lambda') = \sum_{|\alpha|=n} b'_\alpha B^n_\alpha(\lambda')$ *be Bézier maps defined with respect to polytopes* P *and* P' *that share a common vertex, edge, or (hyper-)face* $\mathbf{f}$ *(implying that* $\lambda_i(\mathbf{x}) = \lambda'_i(\mathbf{x})$ *for all* i *and* $\mathbf{x} \in \mathbf{f}$*). Let* $\mathbf{f}$ *be determined by its vertices* $V := \{\mathbf{v}_{i_j}\}_{j=1}^l = \{\mathbf{v}'_{i_j}\}_{j=1}^l$. *(Without loss of generality, let corresponding vertices have the same indices.) Assume that, for every multi-index* β *with* $|\beta| = n-1$ *and* $\beta_i = 0$ *if* $i \notin V$, *an affine function* A_β *exists such that* $b_\alpha = A_\beta(\sum_i \frac{\alpha_i}{n}\mathbf{v}_i)$ *and* $b'_\alpha = A_\beta(\sum_i \frac{\alpha_i}{n}\mathbf{v}'_i)$ *for all pairs* α *and* β *such that* $\alpha = \beta + \mathbf{e}_j$.

Then, the derivative of f *and* f' *at points* $\mathbf{x} \in \mathbf{f}$ *with respect to a differential operator* $\partial \in \left\{\frac{\partial}{\partial x_i}\right\}$ *is*

$$\partial f(\lambda(\mathbf{x})) = \partial f'(\lambda'(\mathbf{x})) = \sum_{\substack{|\beta|=n-1\\ i\notin V \Rightarrow \beta_i=0}} \partial A_\beta \cdot B^{n-1}_\beta(\lambda(\mathbf{x})).$$

Respective statements hold for the higher derivatives of f *and* f'.

Proof. Observe that (2.6) is still valid if not the sum over all β with $|\beta| = n - 1$ is considered but only those β with $\beta_i = 0$ if $i \notin V$ (for $\mathbf{x} \in \mathbf{f}$). This implies the claim. □

For Bézier surfaces, it is often sufficient if the tangent plane varies smoothly without requiring smoothness of the parameterization. In this case, slightly weaker constraints on the control points are sufficient.

2.7 Corollary (Geometric continuity across polytope boundaries). *In the situation of Corollary 2.6 let Q be any affine transformation of the domain $\mathbb{R}^d$ that keeps $\mathbf{f}$ fixed such that $b_\alpha = A_\beta(\sum_i \frac{\alpha_i}{n}\mathbf{v}_i)$ and $b'_\alpha = A_\beta Q(\sum_i \frac{\alpha_i}{n}\mathbf{v}'_i)$ for all pairs α and β such that $\alpha = \beta + \mathbf{e}_j$ and $\beta_i = 0$ if $i \notin V$.*

Then $\partial f(\lambda) = \partial f'(\lambda') \cdot \partial Q$.

Proof. Factoring out Q in (2.6) yields the claim. □

3 Applications

In this section, we present several applications of mean value Bézier maps. Although the results obtained in the previous chapter are general and hold for any barycentric coordinates, Wachspress and mean value coordinates are the only known positive three-point coordinates [4]. Wachspress coordinates, however, have already been used to some extent in the past in the form of tensor product Bézier maps (with parallelepipeds as domain) and S-patches [15] (with regular k-gons as domain). Therefore, it seemed more appropriate to us to use mean value Bézier maps to demonstrate our results.

In all our applications, we begin by specifying several domain polytopes and their respective control points to achieve a smooth Bézier map $f : \mathbb{R}^d \to \mathbb{R}^e$. To determine the polytope in which a point $\mathbf{x} \in \mathbb{R}^d$ lies, we can use another property of mean value coordinates: the mean value coordinates with respect to a polytope P are defined in the whole space $\mathbb{R}^d$ and the denominator (for normalization) in the construction is positive if and only if $\mathbf{x}$ lies within P [8, 13]. Thus, we can automatically determine the polytope P containing $\mathbf{x}$ when computing the mean value coordinates of $\mathbf{x}$ with respect to P.

3.1 Bézier curves and surfaces

If we choose $d = 1$ or $d = 2$ and $e > d$, Bézier maps specialize to Bézier curves and surfaces. In the case $d = 1$, however, barycentric coordinates on the unique 1-dimensional polytope, which is the 1-simplex or line segment, are uniquely determined (t and $1 - t$ on $[0, 1]$). Our results coincide with the well-known theory for Bézier curves.

Therefore, we present an example of a mean value Bézier surface, that is a mean value Bézier map $f : \mathbb{R}^2 \to \mathbb{R}^3$. Figure 3.1 shows a C^1-continuous Bézier surface from several viewpoints. It consists of two patches of degree 2. The domain is the union of a pentagon and an L-shaped hexagon, which share two common edges. Note that the highlights vary smoothly across these edges. The

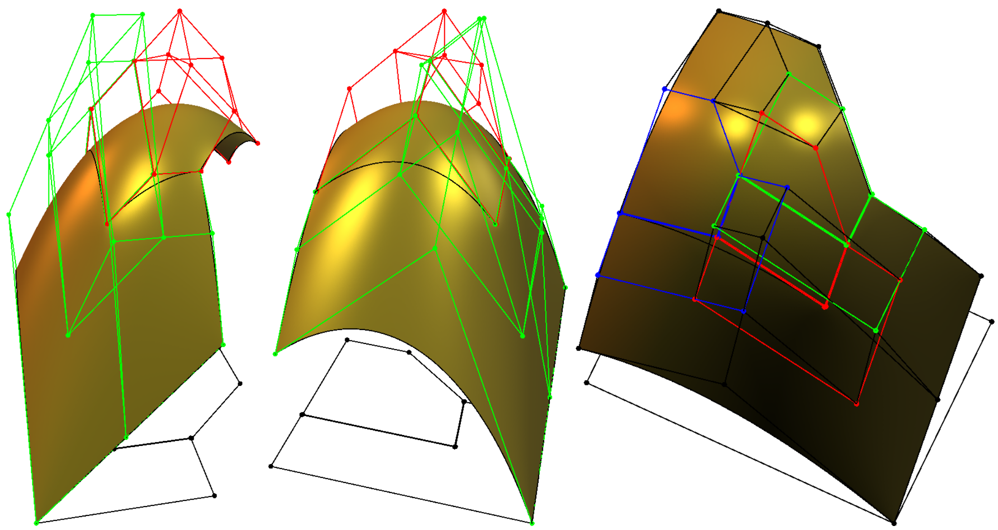

Figure 3.1: Our method makes it possible to use non-convex polygons in the construction of Bézier surfaces. We present three views of a Bézier surface consisting of a pentagonal and an L-shaped hexagonal patch. Note that the highlights vary smoothly across the common edges.

two domain polygons are shown in black below the surface. The control nets, which determine the shape of the surface, are also depicted. We followed the suggestion in [15] and drew all polygons $(b_{\beta+\mathbf{e}_i})_{i=1}^{k}$ with $|\beta| = n - 1 = 1$. (For drawing purposes, we shifted the control net belonging to the pentagon slightly to make sure that it does not overlap with the other one.) On the left and in the middle, we colored the control net for the pentagon red and the control net for the hexagon green. On the right, we chose common colors for the parts of the control net that belong to a common vertex of both polygons. They can be discerned as affine images of the domain.

3.2 Space deformations

A Bézier map with $d = e$ is a space deformation of $\mathbb{R}^d$. While geometric continuity is often sufficient for Bézier curves and surfaces, we need "real" analytic continuity to obtain a smooth space deformation. Even a discontinuity of the absolute value of the derivative in a single direction may be clearly visible if a textured object is deformed.

Figure 3.2 demonstrates a space deformation of $\mathbb{R}^3$. In (a), We show the cuboid that we want to twist by 180°. We align the control polyhedron with the edges of the cuboid. (b) depicts the result if the twist is done directly with mean value coordinates (that is Bernstein polynomials of degree one). The lack of local control leads to a singularity. In (c), we include four additional vertices in the middle of the long edges without changing the total shape of the control polyhedron. This allows us better local control, but C^1-discontinuities are introduced in the middle and at the vertices. (The bead shaped reflection at the top left corner of the cuboid indicates the C^1-discontinuity of mean value coordinates at the vertices.) In (d), we split the control net into two identical, adjoining control polyhedra and deform them independently of each other. This gives us the desired local control but we still have the C^1-discontinuities. In (e), we use a Bézier map of degree 3 to join the two control polyhedra smoothly. It allows us to enforce C^1-continuity while maintaining local control. Observe that also the C^1-discontinuities at the vertices have vanished. The control net shows how the continuity conditions are satisfied here. The left-most and right-most part is an affine image of the domain cuboids to make the deformation smooth at the respective vertices. (The left part is identically mapped, and the right part is rotated by 180° degree.) The two middle "columns" are mapped by a common affine map (both are rotated by 90° degree) to ensure a smooth transition between the adjoining control polyhedra.

Figure 3.3 shows how a complex model can be handled by specifying a control net that is adapted to the shape of the model. It also shows that Bézier maps of different degrees can be mixed under certain circumstances. (Here, the body is mapped identically.) While the body and left front leg is mapped by a degree one map, the Bézier maps for the head and the right leg have degree three.

To display a control polyhedron P, we note that each set $(b_{\beta+\mathbf{e}_i})_{i=1}^k$ with $|\beta| = n-1$ corresponds naturally to the polyhedron with vertices $(\mathbf{v}_i)_{i=1}^k$. Therefore, we connect control points $b_{\beta+\mathbf{e}_i}$ and $b_{\beta+\mathbf{e}_j}$ if and only if $(\mathbf{v}_i, \mathbf{v}_j)$ is an edge in P.

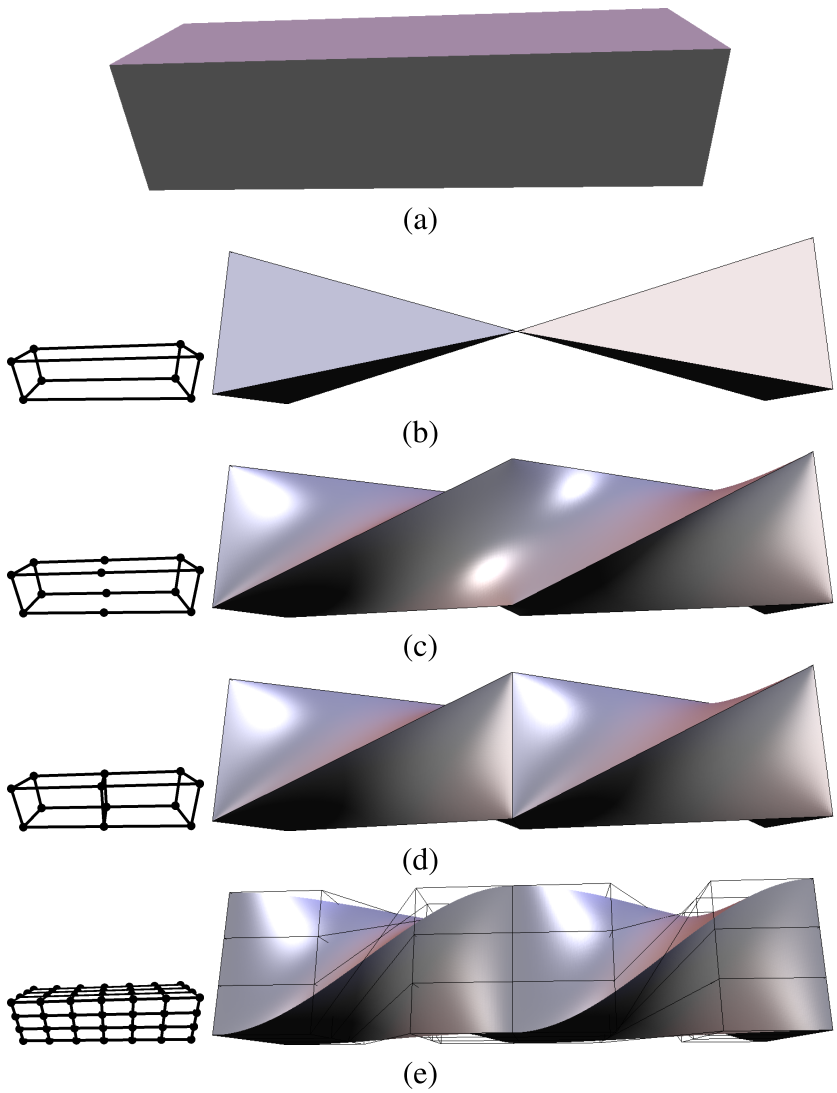

Figure 3.2: A cuboid shall be twisted by 180°. We present results of several methods. The small picture on the left shows the corresponding control net. (a) The undeformed cuboid. (b) Interpolation of the twist with mean value coordinates. (c) Interpolation of the twist with mean value coordinates using additional control points. (d) We split the cuboid into two halves and interpolate both halves with mean value coordinates. (e) Our method. Although we use the same two halves as interpolation domains as in (d), the use of third order polynomials allows us to control the smoothness. If we had increased the number of control points without using higher order polynomials, we would have introduced new discontinuities as in (c) and (d).

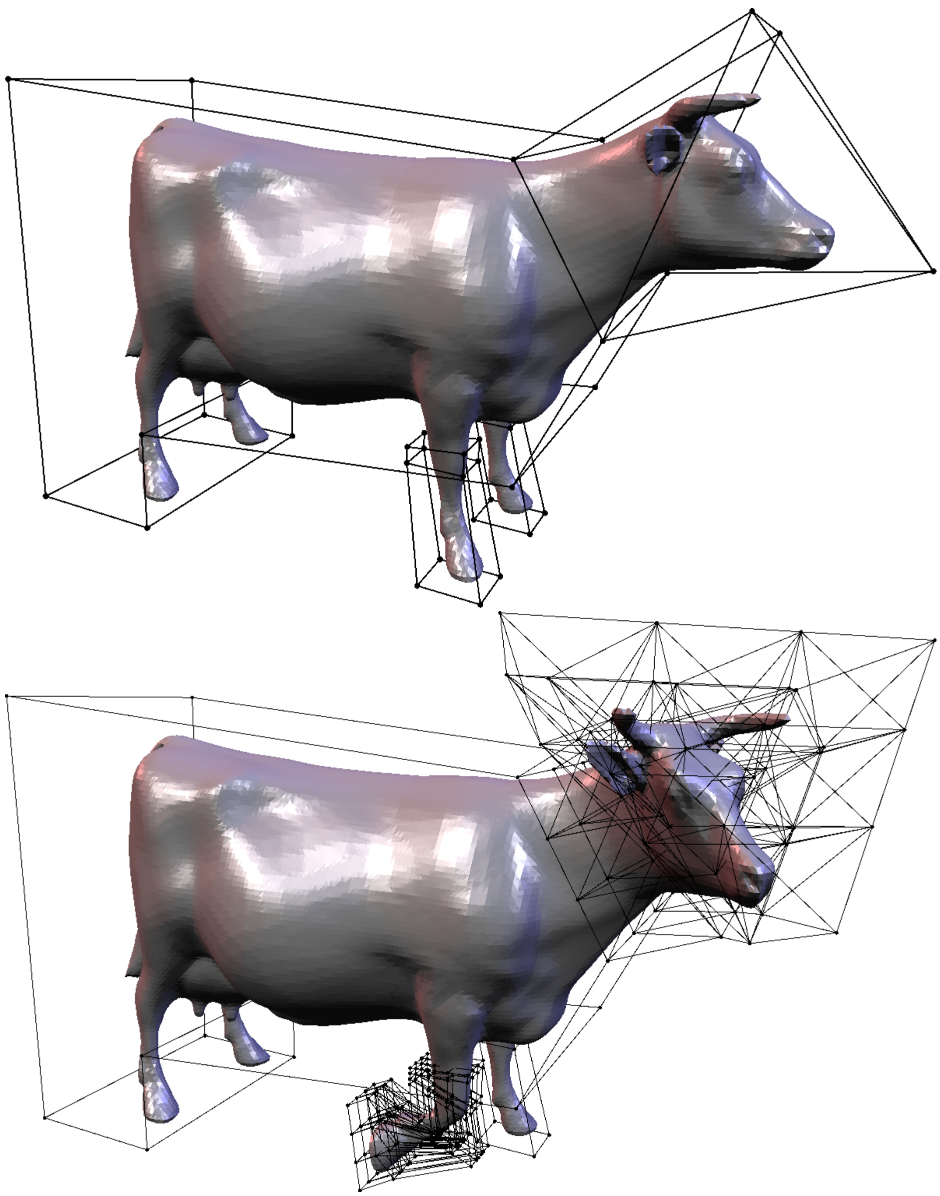

Figure 3.3: The control net containing the cow consists of 6 polyhedra. One for the body, one for the head, two for the front knees, and two for the front legs. It demonstrates the ability of our method to handle complex control nets that are adapted to the shape of the object. We specified the deformation, which is C^1-continuous, by moving the vertices of the control polyhedra shown in the upper row. The intermediate control points, which are depicted in the control net below, were computed automatically.

4 Conclusions and future work

We developed criteria for the construction of smooth Bézier maps. A Bézier map is a map that is piecewise (on a given polytope) a homogeneous polynomial in generalized barycentric coordinates. We showed how the coefficients of the Bernstein polynomials can be chosen to enforce smoothness of any desired order across common (hyper-)faces of the polytopes. We chose to develop the theory in full generality although we mainly aim at Bézier maps in mean value coordinates. This allows the use of our results for any other barycentric coordinates that might come to the focus of attention in the future. Moreover, it shows that many results from the well developed field of simplicial and tensor product Bézier theory can be considered as a special case of our findings if Wachspress coordinates are used. Our indexing scheme, however, does not coincide with the traditional indexing scheme for tensor product Bézier maps. This sheds new light on the classical theory, which will hopefully lead to an better understanding of the tensor product Bézier maps as well.

Probably the most important examples of Bézier maps are Bézier curves and surfaces and space deformations. We presented examples of mean value Bézier surfaces and free-form deformations based on Bernstein polynomials in mean value coordinates as possible applications. Nearly without additional effort, we can ensure that our Bézier maps exhibit the desired smoothness even at the polytope vertices, although the mean value coordinates themselves are only C^0-continuous at these points. Thus, it is now possible to construct smooth mean value Bézier maps with arbitrary polytopes as domains.

Nevertheless, a number of open questions remain, which we intend to address in future work. Foremost, some kind of spline representation of Bézier maps has to be found that takes care of any continuity issues automatically. These splines should allow to place meaningful control points directly during the design of surfaces and deformations without the necessity to spend much time on the cumbersome process of satisfying the continuity constraints manually. Another issue that we did not discuss in the current paper are rational Bézier maps. The use of rational Bézier maps greatly expanded the capabilities of classical Bézier theory. The same should be done for generalized Bézier maps.

Bibliography

[1] P. Bézier. How Renault uses numerical control for car body design and tooling. Paper SAE 680010, Society of Automotive Engineers Congress, Detroit, Mich., 1968.

[2] P. de Casteljau. *Outillage méthodes calcul*. Paris: André Citroën Automobiles S.A., 1959.

[3] M. S. Floater. Mean value coordinates. *Computer Aided Geometric Design*, 20(1):19–27, 2003.

[4] M. S. Floater, K. Hormann, and G. Kós. A general construction of barycentric coordinates over convex polygons. *Advances in Computational Mathematics*, 24(1–4):311–331, Jan. 2006.

[5] M. S. Floater, G. Kós, and M. Reimers. Mean value coordinates in 3D. *Computer Aided Geometric Design*, 22(7):623–631, Oct. 2005. Special Issue on Geometric Modelling and Differential Geometry.

[6] A. R. Forrest. Interactive interpolation and approximation by Bézier polynomials. *Comput. J.*, 15(1):71–79, 1972.

[7] R. Goldman. Multisided arrays of control points for multisided Bézier patches. *Computer Aided Geometric Design*, 21(3):243–261, Mar. 2004.

[8] K. Hormann and M. S. Floater. Mean value coordinates for arbitrary planar polygons. *ACM Transactions on Graphics*, 25(4):1424–1441, Oct. 2006.

[9] T. Ju, P. Liepa, and J. Warren. A general geometric construction of coordinates in a convex simplicial polytope. *Computer Aided Geometric Design*, 24(3):161–178, Apr. 2007.

[10] T. Ju, S. Schaefer, and J. Warren. Mean value coordinates for closed triangular meshes. *ACM Transactions on Graphics*, 24(3):561–566, 2005.

[11] T. Ju, S. Schaefer, J. Warren, and M. Desbrun. A geometric construction of coordinates for convex polyhedra using polar duals. In M. Desbrun and H. Pottmann, editors, *Third Eurographics Symposium on Geometry Processing*, pages 181–186. Eurographics Association, July 2005.

[12] T. Langer, A. Belyaev, and H.-P. Seidel. Spherical barycentric coordinates. In A. Sheffer and K. Polthier, editors, *Fourth Eurographics Symposium on Geometry Processing*, pages 81–88. Eurographics Association, June 2006.

[13] T. Langer, A. Belyaev, and H.-P. Seidel. Mean value coordinates for arbitrary spherical polygons and polyhedra in $\mathbb{R}^3$. In P. Chenin, T. Lyche, and L. L. Schumaker, editors, *Curve and Surface Design: Avignon 2006*, Modern Methods in Mathematics, pages 193–202, Brentwood, TN, 2007. Nashboro Press.

[14] T. Langer and H.-P. Seidel. Mean value Bézier surfaces. In *The Mathematics of Surfaces XII*, 2007. Accepted.

[15] C. T. Loop and T. D. DeRose. A multisided generalization of Bézier surfaces. *ACM Transactions on Graphics*, 8(3):204–234, 1989.

[16] M. Meyer, A. Barr, H. Lee, and M. Desbrun. Generalized barycentric coordinates on irregular polygons. *Journal of Graphics Tools*, 7(1):13–22, 2002.

[17] T. W. Sederberg and S. R. Parry. Free-form deformation of solid geometric models. In *SIGGRAPH '86: Proceedings of the 13th annual conference on Computer graphics and interactive techniques*, pages 151–160, New York, NY, USA, 1986. ACM Press.

[18] E. L. Wachspress. *A Rational Finite Element Basis*, volume 114 of *Mathematics in Science and Engineering*. Academic Press, New York, 1975.

[19] J. Warren. Barycentric coordinates for convex polytopes. *Advances in Computational Mathematics*, 6(2):97–108, 1996.

Below you find a list of the most recent technical reports of the Max-Planck-Institut für Informatik. They are available by anonymous ftp from `ftp.mpi-sb.mpg.de` under the directory `pub/papers/reports`. Most of the reports are also accessible via WWW using the URL `http://www.mpi-sb.mpg.de`. If you have any questions concerning ftp or WWW access, please contact `reports@mpi-sb.mpg.de`. Paper copies (which are not necessarily free of charge) can be ordered either by regular mail or by e-mail at the address below.

Max-Planck-Institut für Informatik
Library
attn. Anja Becker
Stuhlsatzenhausweg 85
66123 Saarbrücken
GERMANY
e-mail: `library@mpi-sb.mpg.de`

MPI-I-2007-5-001	G. Ifrim, G. Kasneci, M. Ramanath, F.M. Suchanek, G. Weikum	NAGA: Searching and Ranking Knowledge
MPI-I-2007-4-001	J. Gall, B. Rosenhahn, H. Seidel	Clustered Stochastic Optimization for Object Recognition and Pose Estimation
MPI-I-2007-2-001	A. Podelski, S. Wagner	A Method and a Tool for Automatic Veriication of Region Stability for Hybrid Systems
MPI-I-2006-5-006	G. Kasnec, F.M. Suchanek, G. Weikum	Yago - A Core of Semantic Knowledge
MPI-I-2006-5-005	R. Angelova, S. Siersdorfer	A Neighborhood-Based Approach for Clustering of Linked Document Collections
MPI-I-2006-5-004	F. Suchanek, G. Ifrim, G. Weikum	Combining Linguistic and Statistical Analysis to Extract Relations from Web Documents
MPI-I-2006-5-003	V. Scholz, M. Magnor	Garment Texture Editing in Monocular Video Sequences based on Color-Coded Printing Patterns
MPI-I-2006-5-002	H. Bast, D. Majumdar, R. Schenkel, M. Theobald, G. Weikum	IO-Top-k: Index-access Optimized Top-k Query Processing
MPI-I-2006-5-001	M. Bender, S. Michel, G. Weikum, P. Triantafilou	Overlap-Aware Global df Estimation in Distributed Information Retrieval Systems
MPI-I-2006-4-010	A. Belyaev, T. Langer, H. Seidel	Mean Value Coordinates for Arbitrary Spherical Polygons and Polyhedra in $\mathbb{R}^3$
MPI-I-2006-4-009	J. Gall, J. Potthoff, B. Rosenhahn, C. Schnoerr, H. Seidel	Interacting and Annealing Particle Filters: Mathematics and a Recipe for Applications
MPI-I-2006-4-008	I. Albrecht, M. Kipp, M. Neff, H. Seidel	Gesture Modeling and Animation by Imitation
MPI-I-2006-4-007	O. Schall, A. Belyaev, H. Seidel	Feature-preserving Non-local Denoising of Static and Time-varying Range Data
MPI-I-2006-4-006	C. Theobalt, N. Ahmed, H. Lensch, M. Magnor, H. Seidel	Enhanced Dynamic Reflectometry for Relightable Free-Viewpoint Video
MPI-I-2006-4-005	A. Belyaev, H. Seidel, S. Yoshizawa	Skeleton-driven Laplacian Mesh Deformations
MPI-I-2006-4-004	V. Havran, R. Herzog, H. Seidel	On Fast Construction of Spatial Hierarchies for Ray Tracing
MPI-I-2006-4-003	E. de Aguiar, R. Zayer, C. Theobalt, M. Magnor, H. Seidel	A Framework for Natural Animation of Digitized Models
MPI-I-2006-4-002	G. Ziegler, A. Tevs, C. Theobalt, H. Seidel	GPU Point List Generation through Histogram Pyramids
MPI-I-2006-4-001	A. Efremov, R. Mantiuk, K. Myszkowski, H. Seidel	Design and Evaluation of Backward Compatible High Dynamic Range Video Compression
MPI-I-2006-2-001	T. Wies, V. Kuncak, K. Zee, A. Podelski, M. Rinard	On Verifying Complex Properties using Symbolic Shape Analysis
MPI-I-2006-1-007	H. Bast, I. Weber, C.W. Mortensen	Output-Sensitive Autocompletion Search
MPI-I-2006-1-006	M. Kerber	Division-Free Computation of Subresultants Using Bezout Matrices
MPI-I-2006-1-005	A. Eigenwillig, L. Kettner, N. Wolpert	Snap Rounding of Bzier Curves
MPI-I-2006-1-004	S. Funke, S. Laue, R. Naujoks, L. Zvi	Power Assignment Problems in Wireless Communication

MPI-I-2005-5-002	S. Siersdorfer, G. Weikum	Automated Retraining Methods for Document Classification and their Parameter Tuning
MPI-I-2005-4-006	C. Fuchs, M. Goesele, T. Chen, H. Seidel	An Emperical Model for Heterogeneous Translucent Objects
MPI-I-2005-4-005	G. Krawczyk, M. Goesele, H. Seidel	Photometric Calibration of High Dynamic Range Cameras
MPI-I-2005-4-005	M. Goesele	?
MPI-I-2005-4-004	C. Theobalt, N. Ahmed, E. De Aguiar, G. Ziegler, H. Lensch, M.A. Magnor, H. Seidel	Joint Motion and Reflectance Capture for Creating Relightable 3D Videos
MPI-I-2005-4-003	T. Langer, A.G. Belyaev, H. Seidel	Analysis and Design of Discrete Normals and Curvatures
MPI-I-2005-4-002	O. Schall, A. Belyaev, H. Seidel	Sparse Meshing of Uncertain and Noisy Surface Scattered Data
MPI-I-2005-4-001	M. Fuchs, V. Blanz, H. Lensch, H. Seidel	Reflectance from Images: A Model-Based Approach for Human Faces
MPI-I-2005-2-004	Y. Kazakov	A Framework of Refutational Theorem Proving for Saturation-Based Decision Procedures
MPI-I-2005-2-003	H.d. Nivelle	Using Resolution as a Decision Procedure
MPI-I-2005-2-002	P. Maier, W. Charatonik, L. Georgieva	Bounded Model Checking of Pointer Programs
MPI-I-2005-2-001	J. Hoffmann, C. Gomes, B. Selman	Bottleneck Behavior in CNF Formulas
MPI-I-2005-1-008	C. Gotsman, K. Kaligosi, K. Mehlhorn, D. Michail, E. Pyrga	Cycle Bases of Graphs and Sampled Manifolds
MPI-I-2005-1-007	I. Katriel, M. Kutz	A Faster Algorithm for Computing a Longest Common Increasing Subsequence
MPI-I-2005-1-003	S. Baswana, K. Telikepalli	Improved Algorithms for All-Pairs Approximate Shortest Paths in Weighted Graphs
MPI-I-2005-1-002	I. Katriel, M. Kutz, M. Skutella	Reachability Substitutes for Planar Digraphs
MPI-I-2005-1-001	D. Michail	Rank-Maximal through Maximum Weight Matchings
MPI-I-2004-NWG3-001	M. Magnor	Axisymmetric Reconstruction and 3D Visualization of Bipolar Planetary Nebulae
MPI-I-2004-NWG1-001	B. Blanchet	Automatic Proof of Strong Secrecy for Security Protocols
MPI-I-2004-5-001	S. Siersdorfer, S. Sizov, G. Weikum	Goal-oriented Methods and Meta Methods for Document Classification and their Parameter Tuning
MPI-I-2004-4-006	K. Dmitriev, V. Havran, H. Seidel	Faster Ray Tracing with SIMD Shaft Culling
MPI-I-2004-4-005	I.P. Ivrissimtzis, W.-. Jeong, S. Lee, Y.a. Lee, H.-. Seidel	Neural Meshes: Surface Reconstruction with a Learning Algorithm
MPI-I-2004-4-004	R. Zayer, C. Rssl, H. Seidel	r-Adaptive Parameterization of Surfaces
MPI-I-2004-4-003	Y. Ohtake, A. Belyaev, H. Seidel	3D Scattered Data Interpolation and Approximation with Multilevel Compactly Supported RBFs
MPI-I-2004-4-002	Y. Ohtake, A. Belyaev, H. Seidel	Quadric-Based Mesh Reconstruction from Scattered Data
MPI-I-2004-4-001	J. Haber, C. Schmitt, M. Koster, H. Seidel	Modeling Hair using a Wisp Hair Model
MPI-I-2004-2-007	S. Wagner	Summaries for While Programs with Recursion
MPI-I-2004-2-002	P. Maier	Intuitionistic LTL and a New Characterization of Safety and Liveness
MPI-I-2004-2-001	H. de Nivelle, Y. Kazakov	Resolution Decision Procedures for the Guarded Fragment with Transitive Guards
MPI-I-2004-1-006	L.S. Chandran, N. Sivadasan	On the Hadwiger's Conjecture for Graph Products
MPI-I-2004-1-005	S. Schmitt, L. Fousse	A comparison of polynomial evaluation schemes